ELSEVIER

Catalysis Today 72 (2002) 213–221

CATALYSIS TODAY

www.elsevier.com/locate/cattod

Plasma-chemical synthesis and regeneration of catalysts for reforming natural gas

G.P. Vissokov [a], M.I. Panayotova [b,*]

[a] *Institute of Electronics, Bulgarian Academy of Sciences, 72 Tsarigradsko Chaussee Blvd., 1784 Sofia, Bulgaria*
[b] *Department of Chemistry, University of Mining and Geology, 1100 Sofia, Bulgaria*

Abstract

This study describes a pioneering investigation of plasma-chemical synthesis (PCS) and/or regeneration of natural gas-reforming catalysts under the conditions of electric arc, low temperature plasma (LTP), as a function of plasma-chemical process (PCP) parameters and plasma-chemical reactor (PCR) type (with "cold walls" or "warm walls"). Based on the model calculations, a plasma-chemical installation was designed, built, and used to study the processes of catalyst preparation and regeneration of spent, deactivated catalysts for natural gas-reforming.

Plasma-chemically synthesized and/or regenerated samples were analyzed by means of complex physical-chemical, X-ray pattern structural, and electron-microscopic analyses. And the dynamics and kinetics of active surface formation by reduction of catalysts were studied.

A temperature range of 2000–3000 K has been established as optimal for synthesizing samples with maximum dispersion, producing a reduction rate 2–4 times faster than industrial analogues. Samples with high catalytic activity (CH_4 conversion rate, catalyst performance, catalyst efficiency) and thermal stability were obtained.

Thus, it has been found that LTP can be successfully used for catalyst synthesis and regeneration. © 2002 Elsevier Science B.V. All rights reserved.

Keywords: Plasma-chemical synthesis and regeneration; Catalysts for natural gas-reforming

1. Introduction

Steam-conversion of methane represents an important industrial task, and it is well known that Ni-bearing catalysts aid the process. Such commercial catalysts are prepared and regenerated by different chemical and physicochemical methods.

The two main trends in plasma-chemical synthesis (PCS) of catalysts are (i) plasma-chemical preparation and activation of catalysts in the condensed-phase and (ii) plasma-assisted deposition of catalytically active compounds and composites on various carriers.

The plasma can be employed only to disperse and activate the catalytic substances, or the catalysts are synthesized during the plasma-chemical process (PCP). Furthermore, the ingredients are introduced in jet plasma-chemical reactors (PCR) either as a well-homogenized mechanical mixture of micron-size particles [1–5], or as concentrated solutions and suspensions [6,7]. The plasma-chemical technique is also used for activation of spent deactivated catalysts [1–5,8].

Condensed-phase catalyst preparation can be carried out either under equilibrium (quasi-equilibrium) and non-equilibrium conditions.

However, the patent, periodic, and monographic literature available lacks data on the PCS and

* Corresponding author. Fax: +359-2-9753-201.
E-mail address: tfp@adm1.uctm.edu (M.I. Panayotova).

0920-5861/02/$ – see front matter © 2002 Elsevier Science B.V. All rights reserved.
PII: S0920-5861(01)00495-3

regeneration of catalysts for natural gas-reforming. A survey of the specialized reference literature also reveals an absence of data on equilibrium parameters for the multi-component Ni–Al–O–Ca–Mg system used to build conventional catalysts for natural gas-reforming in the 1000–6000 K temperature range.

The work described in this paper is based on our previous pioneering investigations of PCS and/or regeneration of spent catalysts for ammonia synthesis [9–12], which were addressed by Kizling and Järås [8], and was aimed at the following.

1. Finding the equilibrium concentrations in the Ni–Al–O–Ca–Mg system, at different temperatures (in the range of 1000–6000 K) and at a pressure of 0.1 MPa, to determine the optimum theoretical temperature interval for the PCS of catalysts for methane conversion.
2. Predicting the PCR dimensions and operating conditions.
3. Using the PCP to synthesize materials similar in composition to the commercial G56A catalyst.
4. Comparing the catalytic activity of G56A and the plasma-synthesized catalysts.
5. Pointing out the opportunity to use plasma technology for regeneration of spent catalysts.

2. Calculations

The calculations were based on the fact that the free energy of a chosen system reaches an extremum at equilibrium. Gaseous and condensed-phase compounds, as well as solid solutions were considered, and the potential of electrostatic ionic interaction was taken into account. The set of equations used in the thermodynamic calculations is presented elsewhere [5].

The equilibrium concentrations in the Ni–Al–O–Ca–Mg system were calculated within the 1000–6000 K interval (step of 300 K), at pressure of 0.1 MPa, and with an initial blend content given in Table 1.

The analysis of results for the three different initial contents revealed that, at temperatures above 3100 K, AlO and CaO exist mainly in the gaseous phase. Further, in the range of 3200–3700 K, $CaO{\cdot}2Al_2O_3$ and Al_2O_3 are expected to be in the condensed-phase, depending on the molar (mass) component ratio in the initial Ni–Al–O–Ca–Mg system. Thermodynamic calculations for temperatures between 3700 and 6000 K indicated that all components would be in the gaseous phase, in the form of radicals, atoms (molecules) of the respective elements, and ions and electrons. However, because this study focused on condensed-phase products, specific results in the 3700–6000 K range are not reported, and we did not consider the thermodynamic probability for formation of condensed-phase $NiO{\cdot}Al_2O_3$ (spinel) type although this phase was experimentally observed both in the synthesis and the regeneration of the catalyst samples, and was confirmed by the X-ray pattern analysis.

A three-dimensional model of the motion, heating, melting, and evaporation (thermal destruction) of micron-size particles in an axial-symmetric PCR was developed in order to predict dimensions of the PCR [14]. This model involves a set of partial differential equations that account for the reactor's geometrical parameters, the temperature and velocity profiles inside it, as well as the pressure, viscosity, density, and radial heating of the plasma in the PCR. The equations were solved by means of the flux-corrected transport technique [13,14].

The trajectories of motion of Al and Ni particles with equivalent diameters of 10, 20, 30, 40, 50, and 60 μm were calculated for a PCR. Values used in the calculations are presented in Table 2.

Based on the results of the model calculations, we concluded that an axial-symmetric "cold walls" (CW) or "warm walls" (WW) PCR can be used with the following dimensions: diameter $D_{PCR} = 2$ cm, length $Z_{PCR} = 10$ cm, with ingredients fed radially 1 cm from the plasmatron nozzle. The

Table 1
Variants of initial ingredient concentration in the blend used to calculate the equilibrium concentration of the Ni–Al–O–Ca–Mg system

Ni (mol kg^{-1})	Ni (mass%)	Al (mol kg^{-1})	Al (mass%)	O_2 (mol kg^{-1})	O_2 (mass%)	Ca (mol kg^{-1})	Ca (mass%)	Mg (mol kg^{-1})	Mg (mass%)
2.00020	11.74	14.7720	39.72	26.023	41.64	1.42020	5.69	0.50004	1.21
0.42135	4.47	3.1012	8.37	54.819	87.71	0.29917	1.20	0.10534	0.25
0.04738	0.28	0.2478	0.94	61.640	98.62	0.03364	0.13	0.01844	0.04

Table 2
Values used in the three-dimensional model calculations

Element	Parameter						
	Melting temperature (K)	Boiling temperature (K)	Density at 293 K ($g\,cm^{-3}$)	Density at 1273 K ($g\,cm^{-3}$)	Specific heat capacity ($J\,kg^{-1}\,K^{-1}$)	Standard enthalpy of melting ($kJ\,kg^{-1}$)	Standard enthalpy of vaporization ($kJ\,kg^{-1}$)
Al	933	2725	2.6989	2.289	901.85	403.7	11.19
Ni	1728	3173	8.9	–	444.7	298.2	6.3

device can operate efficiently with particles less than 20 μm in size, and with Ar as plasma-forming gas.

3. Experimental

Based on results of the model and thermodynamic calculations, we built the plasma-chemical installation shown in Fig. 1 [5].

Because the investigation reported here was not preceded by any similar studies, our initial efforts were directed at exploring the simple Ni–O–Al system, with powder elemental Al and Ni and technical grade O_2 used as initial raw materials. Because the blend comprises components of varying bulk masses, a piston powder-feeding device was used for powder-feeding, which prevented separation of ingredients during the powder-feeding process. Consumption of the powder ingredients took place at 2–3 $g\,min^{-1}$ depending on

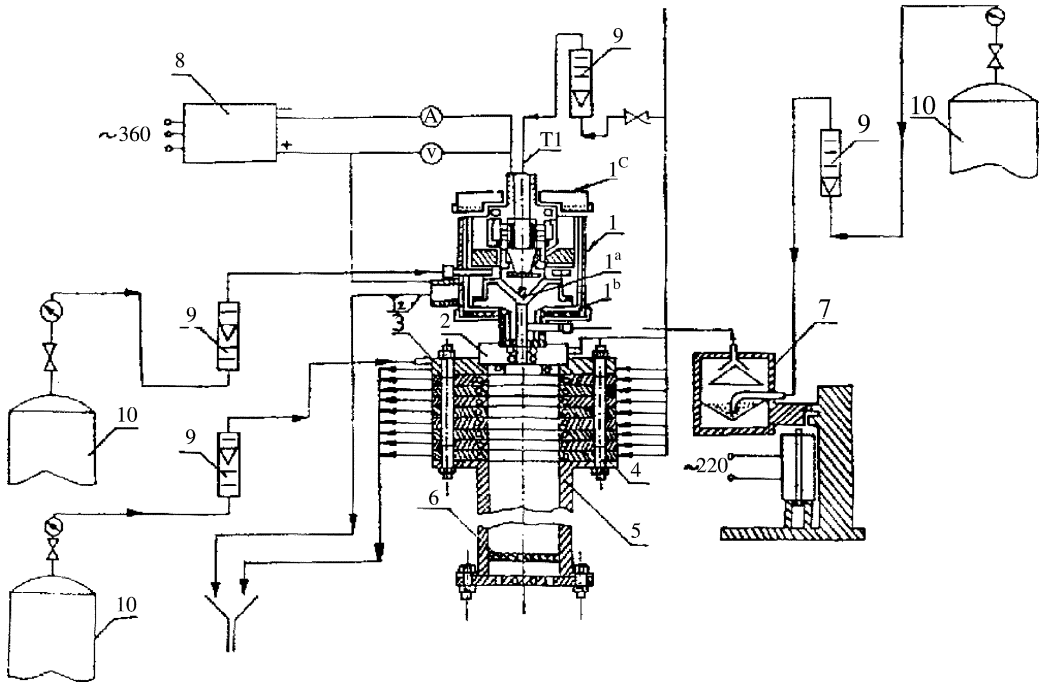

Fig. 1. Schematic drawing of the plasma-chemical installation for synthesis and regeneration of catalysts. 1: electric-arc dc plasmatron; 1^a: thoriated tungsten cathode; 1^b: copper water-cooled anode; 1^c: plastic adjusting ring; 2: CW PCR; 3: quenching device; 4: copper water-cooled sections for the quenching device; 5: powder-trapping chamber; 6: filter; 7: vibration powder-feeding device (if necessary, a piston type vibration powder-feeding device can also be used); 8: current rectifier; 9: flow-meters; 10: bottles with plasma-forming, powder carrying and quenching gases; T_1: temperature of inlet water; T_2: temperature of outlet water.

Table 3
Conditions for obtaining MPCSC

Catalyst type	Parameter					
	Acronym	Type of PCR	Temperature in the PCR (K)	Raw material composition		
				Ni:Al mass ratio	CaO	MgO
Metal plasma-chemically synthesized catalyst in PCR with "cold walls"	MPCSCCW	CW	1100–2400	1:5.5	Present in the reactor	Present in the reactor
Metal plasma-chemically synthesized catalyst in PCR with "warm walls"	MPCSCWW	WW	1200–2700	1:5.5	Present in the reactor	Present in the reactor

the amount of the powder-carrying gas and on the piston revolution rate of the vibrating, powder-feeding device; the equipment's output was within the range of 100–150 g h^{-1}. Argon was used as plasma-forming gas at consumption rate of 1.19 g s^{-1}, while O_2 (flow of 0.29 g s^{-1}) was both powder-carrier and oxidizing agent. The plasma current was kept constant (400 A) throughout the experiment, whereas the discharge voltage was varied within narrow limits (23.5–26 V) by means of changing the cathode–anode distance using the adjustable ring of the plasmatron.

Catalyst samples were synthesized under varying conditions, as described in Tables 3 and 4. The experiments were carried out in one PCR with "cold walls" and one with "warm walls". Technical Ar with a specific flow of 0.89 g s^{-1} was used as plasma-forming gas; technical O_2 with flow of 0.25 g s^{-1} was used as powder-carrier and, in some cases, as oxidizing agent.

The samples of catalysts were characterized by their specific surface area (measured using the BET technique), density, and chemical content. Spectral emission, derivatographic, X-ray pattern, electron-microscopic, etc. analyses were performed.

The dynamics and kinetics of sample reduction were followed using the flow technique. The reduction of the samples was carried out with 1 cm^3 of catalyst at a volume rate of the reducing agent (technical grade H_2) of 40,000 h^{-1} under low temperature plasma (LTP) conditions.

The investigation of the catalytic activity of the PCS materials was performed in a line plant (Fig. 2) for natural gas-reforming at a pressure of 0.1 MPa; at volume rates of dry natural gas of 2000, 5000, 7500, 10,000, 15,000, and 20,000 h^{-1}; within the temperature range of 873–1073 K; and at a steam/gas ratio of 2:1, corresponding to a temperature of 360 K in the steam–gas saturator. Upon CH_4 steam-conversion, the following two reactions were running:

$$CH_4 + H_2O \rightarrow CO + 3H_2 - 206\,kJ \quad (1)$$

$$CO + H_2O \rightarrow CO_2 + H_2 + 41\,kJ \quad (2)$$

The summarized reaction may be presented as follows:

$$CH_4 + 2H_2O \rightarrow CO_2 + 4H_2 - 165\,kJ \quad (3)$$

Analysis of the converted steam–gas mixture was performed in an "Orsa" gas-analyzer. The content of CO_2, CO, and O_2 was determined, and the H_2 content was calculated according to the above-mentioned

Table 4
Conditions for obtaining OPCSC

Catalyst type	Parameter						
	Acronym	Type of PCR	Temperature in the PCR (K)	Raw material composition mass%			
				Al_2O_3	NiO	CaO	MgO
Oxide plasma-chemically synthesized catalyst in PCR with "cold walls"	OPCSCCW	CW	1000–1800	75	15	8	0.2
Oxide plasma-chemically synthesized catalyst in PCR with "warm walls"	OPCSCWW	WW	1400–3400	75	15	8	0.2

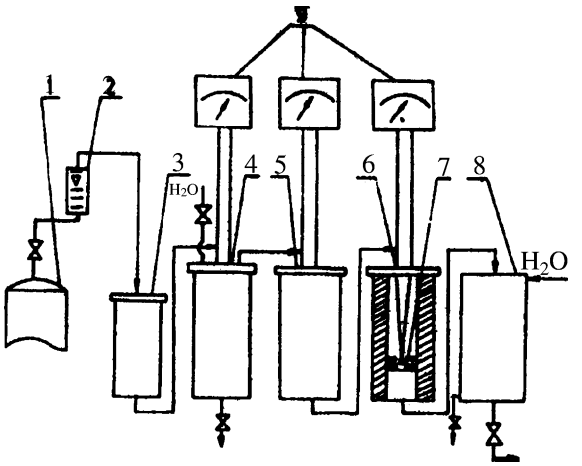

Fig. 2. Schematic drawing of the natural gas-reforming plant. 1: bottle of natural gas (95% CH_4); 2: gas flow-meter; 3: apparatus for sulfuric compounds removal from the gas; 4: steam–gas saturator; 5 and 6: catalytic reactor with thermocouples; 7: catalyst layer; 8: condenser-cooler; 9: temperature measuring devices.

reactions. The remainder (to 100%) was assumed to be unreacted CH_4.

The main process parameter of the natural gas-reforming process is the CH_4 conversion rate:

$$\eta\,(\%) = \left[\frac{(V_{\mathrm{CH_4\,input}} - V_{\mathrm{CH_4\,output}})}{V_{\mathrm{CH_4\,input}}}\right] \times 100 \qquad (4)$$

where $V_{\mathrm{CH_4\,input}}$ is the CH_4 volume input in the reactor under normal conditions (m^3); and $V_{\mathrm{CH_4\,output}}$ is the CH_4 volume output of the reactor under normal conditions (m^3).

Catalyst performance is presented as follows:

$$G\,(\mathrm{m^3_{(H_2+CO)}\,m^{-3}_{cat}}) = \frac{V_{(\mathrm{H_2+CO})}}{V_{\mathrm{cat}}} \qquad (5)$$

where, $V_{(\mathrm{H_2+CO})}$ is the volume of $H_2 + CO$ quantities formed under normal conditions (m^3); and V_{cat} is the catalyst volume (m^3).

Catalyst efficiency represents a relationship between the practical CH_4 steam-conversion ratio and the equilibrium ratio:

$$\eta_{\mathrm{ef}} = \frac{\eta}{\eta_{\mathrm{equil}}} \qquad (6)$$

where η is the empirically determined conversion ratio (%) and η_{equil} is the equilibrium ratio.

4. Results and discussion

Table 5 summarizes some technological parameters and properties of the products of plasma-chemical treatment of the Ni–O–Al system.

Results of the X-ray pattern analysis (Fig. 3) show that the PCS samples are made of NiO, α-Al_2O_3, and $NiAl_2O_4$. For comparison, X-ray patterns of fresh and deactivated G56A catalyst are shown in Fig. 4.

The electron microscopy (Fig. 5) revealed that particles produced were nearly spherical in shape and their equivalent diameters fell within the range of 10–30 nm.

The extent to which the degree of reduction depended on time is presented in Fig. 6 for sample number 5 (Table 5) and for fresh G56A catalyst. The extent to which the degree of reduction of the oxide PCS catalysts (OPCSC) and the fresh G56A catalyst depended on time is shown in Fig. 7.

The metal PCS catalysts (MPCSC) sample was almost totally reduced within 4 h (the temperature was raised from 473 to 573 K for 1.5 h), whereas under the

Table 5
Technological parameters and properties of the products of plasma-chemical treatment of the Ni–O–Al system with a plasma-forming gas (Ar) flow of 0.19 g s^{-1} and powder-carrying gas (O_2) flow of 0.29 g s^{-1}

Number	I (A)	U (V)	W (kW)	T_{pl} (K)	H_{p} (kJ kg^{-1})	T_{R} (K)	Ni (%)	Al_2O_3 (%)	ρ (kg m^{-3})	S (m^2 g^{-1})
1	400	26	10.4	6350	3310	3610	14.3	78.9	130	122
2	400	26	10.4	6210	3220	3470	5.5	85.6	110	107
3	400	26	10.4	6220	3220	3480	6.0	84.9	140	117
4	400	25.5	10.2	5400	2800	3100	13.7	80.0	140	119
5	400	25.5	10.2	5400	2800	3200	12.7	78.3	130	108
6	400	25	10.0	4860	2540	3020	7.3	82.4	140	115
7	400	23.5	9.4	4220	2240	2880	7.9	86.2	130	119

T_{pl}: average plasma temperature; T_{R}: average reactor temperature; H_{p}: average plasma enthalpy.

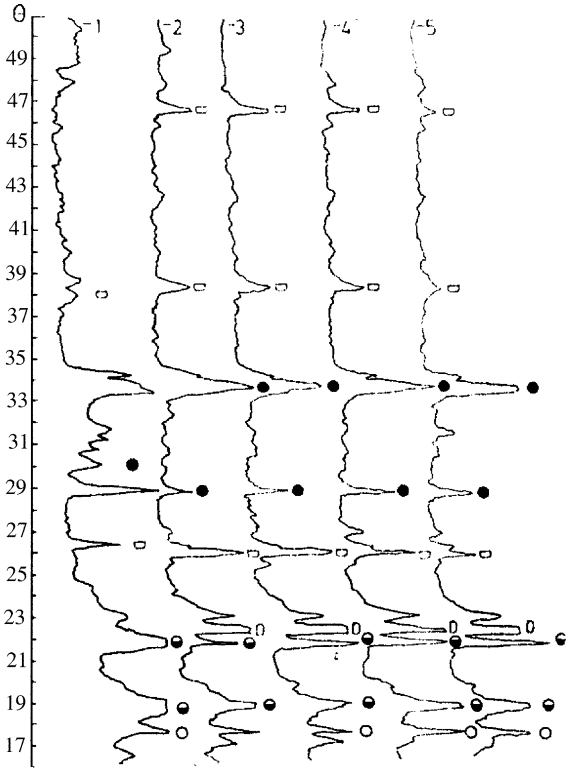

Fig. 3. X-ray patterns of catalysts type OPCSCCW and G56A. 1: G56A; 2: OPCSCCW-1; 3: OPCSCCW-2; 4: OPCSCCW-3; 5: OPCSCCW-4; numbers correspond to samples shown in Table 5; (◒): NiO; (○): Al_2O_3; (●): $NiAl_2O_4$; (▭): N; (▯): Al.

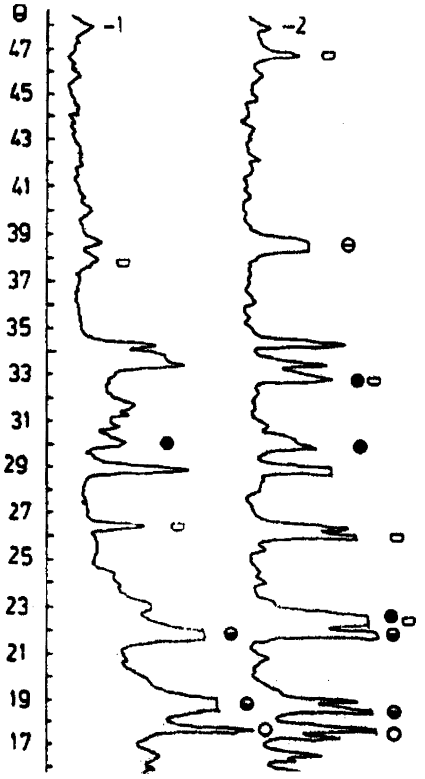

Fig. 4. X-ray patterns of catalysts for natural gas-reforming. 1: fresh catalyst type G56A; 2: deactivated catalyst type G56A; (◒): NiO; (○): Al_2O_3; (●): $NiAl_2O_4$; (▭): N.

same conditions and duration, the G56A catalyst was reduced by only 25% (Fig. 6). OPCSC samples were completely reduced in 7 h (temperature was increased to 773 K), while under the same conditions and duration, the G56A catalyst reached up to 30% reduction (Fig. 7).

The main portion of H_2O was separated during the initial reduction hours, as can be seen in Figs. 6 and 7, because the reducer (H_2) initially attacks the surface layer of the unreduced catalyst particles. The rate of chemical interaction of H_2 and NiO limits the process rate, at low temperatures (up to 673 K), i.e. the process takes place in the kinetic region. As the process progresses to the depth of G56A catalyst particles, reverse diffusion of steam from the particles' depth to the surface impedes the process rate.

Within the induction period of reduction, a new phase of elemental Ni starts forming and catalyses

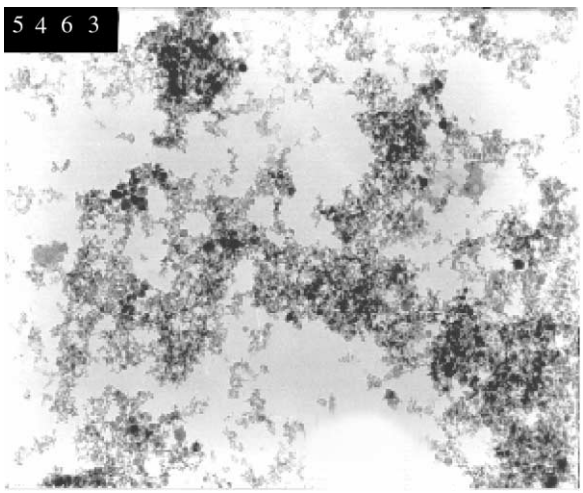

Fig. 5. Electron microscope photograph of sample number 1, Table 5; magnification 36,000, 1 mm = 28 nm.

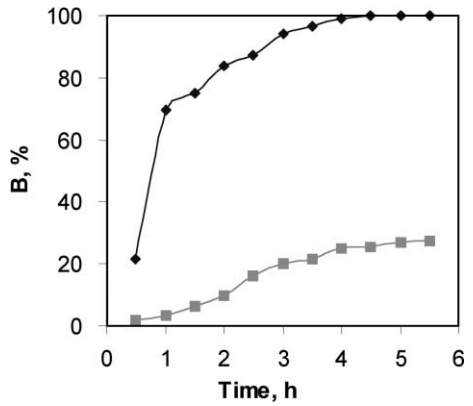

Fig. 6. Reduction degree (B, %) of MPCSC and G56A catalyst samples as a function of time (τ, h). (◆): MPCSC; (■): G56A.

the natural gas-reforming process. Within the second period (self-catalyzing), nuclei from the new elemental Ni phase are already formed, as the reduction process is significantly eased and its rate is increased due to the increase in boundary surface between the phases (Ni and Al_2O_3). At the end of the process (supplementary reduction), the quantity of H_2O formed decreases to zero and the reduction degree reaches constant value, indicating completion of the process.

Our experiments highlighted the difficulty of reaching, in real time, 100% reduction of the commercial G56A catalyst. This difficulty may be explained by the presence of concentrated solid solutions of the promoters (CaO, MgO, Al_2O_3) with NiO or $NiAl_2O_4$ in the catalyst, which, as the reduction approaches its end (degree of reduction: ≥90%), may substantially hamper further catalyst reduction.

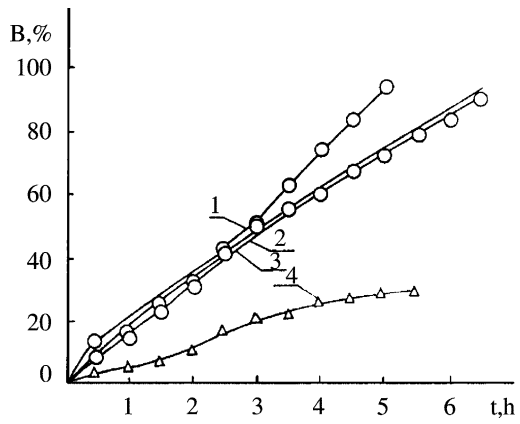

Fig. 7. Reduction degree (B, %) of OPCSC and G56A catalyst samples as a function of time (τ, h). 1: OPCSC-1; 2: OPCSC-2; 3: OPCSC-3; numbers correspond to samples shown in Table 5; 4: G56A.

Reasons for a three-fold increase in reduction rate for the PCS catalyst compared to the G56A industrial catalyst include the following.

1. The sample, obtained under the conditions of electric-arc LTP, has a specific surface of $108\,m^2\,g^{-1}$, while that of the G56A catalyst is $4\,m^2\,g^{-1}$. A highly developed surface is essential to the intensive transport of hydrogen molecules into the sample's pores, and thus, intensifies the overall reduction process (when the latter is diffusion controlled).
2. The presence of promoters in the industrial catalysts slows down its reduction by blocking the transport capillaries.

Results from the investigations of the catalytic activity of MPCSC in a PCR with "cold walls" (MPCSCCW) are presented in Table 6.

The summarized results revealed that OPCSC in a PCR with "cold walls" (OPCSCCW) are similar to G56A in their activity, which indicates that one possible reason for the insufficiently high activity of MPCSCCW and OPCSCCW could be the utilization of a reactor with "cold walls". For that type of reactor, favorable conditions are available for the so-called "wall effect". As a result, the oxidation degree of the ingredients for MPCSC is relatively low, and the blend evaporation for MPCSC and OPCSC is incomplete, as was confirmed by the X-ray structural analysis data.

Table 6
Comparison of catalytic activity in the natural gas-reforming process of commercial G52A and MPCSCCW

Catalyst type	Parameter		
	Natural gas volume rate, V (h^{-1})	Temperature (K)	η_{ef} (%)
G56	500	873	43.6
	5000	973	42.6
MPCSCCW	500	873	38.0
	5000	973	32.1

Table 7
G56A and MPCSCWW catalyst activity in the natural gas-reforming process at 923 K and some main process parameters

Material	Parameter							
	Natural gas volume rate, V (h^{-1})	Converted gas composition (vol.%)				CH_4 conversion rate, η (%)	Catalyst performance[a]	Catalyst efficiency, η_{ef} (%)
		CO_2	CO	H_2	CH_4			
G56A	2000	13.0	3.9	63.7	80.6	80.6	1352	99.5
	5000	11.5	2.4	53.2	67.1	67.1	2780	82.8
	7500	11.2	2.2	51.4	64.8	64.8	4020	80.0
	10000	11.1	2.1	50.7	63.9	63.9	5280	78.9
MPCSCWW	2000	13.0	3.7	63.1	79.8	79.8	1336	98.5
	5000	11.9	2.9	56.3	71.1	71.1	2960	87.8
	7500	11.4	2.5	54.3	69.2	69.2	4260	84.2
	10000	11.3	2.3	52.7	66.3	66.3	5500	81.9

[a] $G \times 10^3$ ($m^3_{(CO+H_2)}\, m^{-3}_{cat}$).

Table 8
Plasma-chemically regenerated and fresh G56A catalyst activity in the CH_4 steam-conversion process at 873 K and some main process parameters

Catalyst type	Natural gas volume rate, V (h^{-1})	Converted gas composition (vol.%)				CH_4 conversion rate, η (%)	Catalyst performance[a]	Catalyst efficiency, η_{ef} (%)
		CO_2	CO	H_2	CH_4			
G56A regenerator	2000	10.1	1.0	43.4	45.5	54.5	888	91.0
G56A fresh	2000	10.2	1.0	43.8	40.0	59.0	896	98.6

[a] $G \times 10^3$ ($m^3_{(CO+H_2)}\, m^{-3}_{cat}$).

In addition, catalyst reduction is required for a highly active catalytic surface to be formed and for the catalyst to evolve into a functional condition. In order to eliminate these disadvantages, we devoted our further investigation to the PCS of metal and oxide catalysts in a reactor with "warm walls".

MPCSC in a PCR with "warm walls" (MPCSCWW) have commensurable and even higher activity compared to the G56A industrial sample (Table 7) when tested under identical conditions (temperature, volume rate, steam/gas ratio).

The high catalytic activity of the PCS catalysts for CH_4 steam-conversion is caused by the high specific surface area of the samples (to 110 $m^2\, g^{-1}$) and the high particle dispersity (10–30 nm), which decreases diffusion limitations. Additional contributors to this high activity include faulty structure and phase composition defined upon condensed-phase forming after plasma-chemical reaction at a quenching rate of $dT/d\tau = 10^4$–$10^5\, K\, s^{-1}$ and NiO homogenous distribution between structure-stabilizing Al_2O_3 and activating CaO. The temperature-resistance of the PCS catalysts was determined by the existence of $NiAI_2O_4$ in the fresh samples.

A comparison of fresh G56A industrial catalyst and catalyst regenerated under the conditions of LTP is presented in Table 8.

5. Conclusion

The technique we employed to calculate the free energy of the multi-component heterogeneous system Ni–Al–O–Ca–Mg enabled us to consider its equilibrium state in the presence of powders, condensed-phase substances, and solid solutions. We were, thus, able to follow a large variety of equilibrium positions, ranging from condensed state to plasma-state of the substances present, and to choose the proper ratios of raw materials for plasma-synthesis of catalysts for

natural gas conversion. We were also able to determine the optimal temperature range of the plasma reactor.

The results of the model calculations for the PCP parameters (PCR size, residence time of the particle in the reactor, temperature and velocity profiles in a "cold walls" or "warm walls" PCR, variation of the temperature and particle diameter along the PCR length) allowed us to choose the optimal PCR parameters and to build the plasma-chemical installation for synthesis and regeneration of catalysts.

We discovered that materials with a controlled structure and phase composition can be produced by controlling the content of raw material introduced in the plasma reactor and parameters of the PCS.

We also found that catalysts synthesized in a "cold walls" PCR (metal and oxide) exhibit similarities to their industrial analogue G56A in their activity in the natural gas-reforming reaction, when the process is performed at natural gas volume rate of 500–5000 h^{-1}. Furthermore, metal catalyst samples synthesized in a PCR with "warm walls" have an activity commensurable to that of G56A at a natural gas volume rate of 2000–3000 h^{-1}. However, at a gas volume rate $\geq$5000 h^{-1}, MPCSC synthesized in a "warm walls" PCR are more active than G56A. Consequently, the catalysts synthesized in a PCR with "warm walls" are more effective than conventional catalysts for natural gas-reforming at a high volume rate of natural gas.

The homogeneous composition of synthesized catalysts, the high rate of active chemical surfaces formation by reduction, the thermal stability, and, primarily, the high catalytic activity make these new catalysts a potential competitor to their industrial analogues upon their intended use.

In addition, it should be noted that the PCP proved to be effective for regenerating spent industrial catalysts.

Acknowledgements

This research was partially subsidized by the National Fund for Scientific Investigations, Contract X 563.

References

[1] G. Vissokov, Commun. Dept. Chem. Bulg. Acad. Sci. 16 (1983) 114.
[2] G. Vissokov, Applied Plasma-Chemistry (Part 1), Tekhnika Publishers, Sofia, 1984, p. 295.
[3] G. Vissokov, Applied Plasma-Chemistry (Part 2), Tekhnika Publishers, Sofia, 1987, p. 325.
[4] G. Vissokov, Commun. Dept. Chem. Bulg. Acad. Sci. 16 (1983) 275.
[5] G. Vissokov, D.Sc. thesis, Sofia, 1994.
[6] P. Tsibulev, D.Sc. thesis, Kiev, 1996.
[7] P. Tsibulev, V. Parhomenko, Katalis and katalizatory, Naukova dumka, Kiev, 1989, p. 17.
[8] M. Kizling, S. Järås, Appl. Catal. A: Gen. 147 (1996) 1.
[9] T. Peev, G. Vissokov, I. Czako-Nagy, A. Vertes, Appl. Catal. 19 (1985) 301.
[10] G. Vissokov, T. Peev, I. Czako-Nagy, A. Vertes, Appl. Catal. 27 (1986) 257.
[11] G. Vissokov, Latv. Khim. Zh. 6 (1992) 662.
[12] G. Vissokov, Latv. Khim. Zh. 3 (1992) 334.
[13] P. Pirgov, G. Vissokov, Khimiya i Industriya (Sofia) 67 (1996) 54.
[14] G. Vissokov, P. Pirgov, in: A. Andreev, L. Petrov, Ch. Bonev, G. Kadinov, I. Mitov (Eds.), Proceedings of the 8th International Symposim on Heterogeneous Catalysis, Varna, September 1996, Academic Publishers, Sofia.